Solvent Dynamical Effects in Electron Transfer: Evaluation of Electronic Matrix Coupling Elements for Metallocene Self-Exchange Reactions

George E. McManis, Roger M. Nielson, Alexander Gochev, and Michael J. Weaver*

Contribution from the Department of Chemistry, Purdue University, West Lafayette, Indiana 47907. *Received January 11, 1989*

Abstract: The functional dependence of the rate constants for self-exchange, k_{ex}, for a series of metallocene redox couples to solvent-induced variations in the nuclear frequency factor, ν_n, engendered by alterations in the longitudinal solvent relaxation time, τ_L, are utilized to deduce values of the electronic matrix coupling element, H_{12}, for electron exchange. The analysis exploits the sensitivity of the k_{ex}–τ_L^{-1} dependence to the degree of reaction adiabaticity and hence H_{12} for a given electron-exchange reaction. Six metallocene couples are examined: $Cp_2Co^{+/0}$, $Cp_2Fe^{+/0}$ (Cp = cyclopentadienyl), the decamethyl derivatives $Cp'_2Co^{+/0}$ and $Cp'_2Fe^{+/0}$ scrutinized previously, with additional solvent-dependent k_{ex} values for (carboxymethyl)cobaltocenium–(carboxymethyl)cobaltocene [$Cp^e_2Co^{+/0}$, e = "ester"] and (hydroxymethyl)ferrocenium–(hydroxymethyl)ferrocene [$HMFc^{+/0}$]. Kinetic data are examined in 15 solvents, including 11 "Debye" solvents for which it is anticipated that $\nu_n \propto \tau_L^{-1}$. Corrections to k_{ex} for the solvent-dependent variations in the barrier height were obtained by corresponding measurements of the optical electron-transfer energies for the related binuclear complex biferrocenylacetylene, yielding "barrier-corrected" rate constants, k'_{ex}. The k'_{ex}–τ_L^{-1} dependencies, as well as the k_{ex} values in a given solvent, are markedly dependent on the redox couple. The log k'_{ex}–log τ_L^{-1} plots for the most facile couple, $Cp'_2Co^{+/0}$, exhibit slopes approaching unity for smaller τ_L^{-1} values. The less facile couples yield smaller slopes, diminishing in the same sequence that k'_{ex} decreases in a given solvent: $Cp'_2Co^{+/0} > Cp^e_2Co^{+/0} > Cp_2Co^{+/0} \gtrsim Cp'_2Fe^{+/0} > Cp_2Fe^{+/0} \gtrsim HMFc^{+/0}$. These findings are consistent with H_{12} decreasing in the same order. Comparison of such rate–solvent friction dependencies with corresponding plots calculated using a combined solvent friction–electron tunneling model yields the following approximate values of the matrix coupling element for reactant "closest approach", H°_{12} (kcal mol^{-1}): $Cp'_2Co^{+/0}$, 1.0; $Cp^e_2Co^{+/0}$, 0.5–1.0; $Cp_2Co^{+/0}$, 0.5; $Cp'_2Fe^{+/0}$, 0.2; $Cp_2Fe^{+/0}$, 0.1; $HMFc^{+/0}$, 0.075. Reasonable concordance is seen with recent theoretical estimates of H°_{12} for $Cp_2Co^{+/0}$ and $Cp_2Fe^{+/0}$. The relationship between H°_{12} and metallocene electronic structure is briefly discussed. The analysis also enables effective solvent relaxation times for adiabatic barrier crossing in non-Debye media, including primary alcohols, to be extracted.

A central fundamental question in electron-transfer chemistry of widespread current interest concerns how the extent of overlap between the donor and acceptor redox orbitals and its role in influencing reaction rates depend upon the electronic properties and spatial configuration. The overlap is described by the electronic matrix coupling element, H_{12}, which determines the extent of resonance splitting of the barrier top.[1,2] This factor exerts a crucial influence upon electron-transfer kinetics, by influencing not only the barrier shape and height but also the degree of reaction adiabaticity (i.e., the probability that electron transfer will occur once the transition state has been formed).[2] Recent ab initio calculations of H_{12} for simple outer-sphere electron-exchange processes illustrate the sensitivity of the coupling strength to electronic structure as well as to the spatial configuration of the reacting pair.[2] While experimental estimates of H_{12} for optical electron transfer within binuclear complexes can be extracted from band intensities,[1a] the evaluation of the matrix coupling element for thermal outer-sphere electron transfer is considerably less straightforward. In spite of the importance of the latter quantity as alluded to frequently in the literature,[1-3] its experimental evaluation has remained largely elusive.[4]

We have recently been examining in detail the solvent-dependent electron-exchange kinetics of various metallocene redox couples in homogeneous solution[5] as well as electrode surfaces[6] in order to explore the role of solvent relaxation dynamics on the barrier-crossing frequencies. Of primary concern have been redox couples of the form $Cp_2M^{+/0}$ or $Cp'_2M^{+/0}$, where M = Co or Fe, Cp = cyclopentadienyl, and Cp' = pentamethylcyclopentadienyl,[5,6] although other metallocene couples have also been examined.[6b,d] During these studies, it became apparent that the rate constants for homogenous self-exchange, k_{ex}, in a given solvent display a marked sensitivity to the metallocene electronic structure. In particular, k_{ex} values for cobaltocenium–cobaltocene couples are substantially (up to ca. 10-fold) larger than for corresponding ferrocenium–ferrocene couples: up to 100-fold enhancements in k_{ex} are observed upon methylation of the Cp rings together with substituting cobalt for iron.[5a,7] These rate variations, especially those resulting from metal substitution, were traced primarily to the greater extent of donor–acceptor orbital overlap for the cobalt versus iron systems anticipated from the primarily ligand- versus metal-centered character of the redox orbitals.[7] These differences in orbital overlap and hence H_{12} are consistent both with optical electron-transfer measurements for biocobaltocene versus biferrocene cations[8] and with recent ab initio calculations (vide infra).[9]

(1) For recent reviews, see: (a) Creutz, C. *Prog. Inorg. Chem.* **1983**, *30*, 1. (b) Sutin, N. *Prog. Inorg. Chem.* **1983**, *30*, 441. (c) Newton, M. D.; Sutin, N. *Annu. Rev. Phys. Chem.* **1984**, *35*, 437.

(2) (a) Newton, M. D. *Int. J. Quantum Chem. Symp.* **1980**, *14*, 363. (b) Newton, M. D. *ACS Symp. Ser.* **1982**, *198*, 255. (c) Newton, M. D. *J. Phys. Chem.* **1986**, *90*, 3734. (d) Newton, M. D. *J. Phys. Chem.* **1988**, *92*, 3049.

(3) For example: (a) Taube, H. *Adv. Chem. Ser.* **1977**, *162*, 127. (b) Brunschwig, B. S.; Creutz, C.; McCartney, D. H.; Sham, T.-K.; Sutin, N. *Faraday Discuss. Chem. Soc.* **1982**, *74*, 113. (c) Ulstrup, J. *Charge Transfer Processes in Condensed Media*; Lecture Notes in Chemistry No. 10; Springer-Verlag, Berlin, 1979; p 122. (d) Brocklehurst, B. *J. Phys. Chem.* **1979**, *83*, 536. (e) Taube, H. In *Tunneling in Biological Systems*; Chance, B., DeVault, D. C., Frauenfelder, H., Marcus, R. A., Schrieffer, J. R., Sutin, N., Ed.; Academic Press, New York, 1979; p 173 (see also other papers and discussion in this volume). (f) Haim, A. *Prog. Inorg. Chem.* **1983**, *30*, 273. (g) Yee, E. L.; Weaver, M. J. *Inorg. Chem.* **1980**, *19*, 1936. (h) Weaver, M. J.; Li, T. T.-T. *J. Phys. Chem.* **1986**, *90*, 3823. (i) Balzani, V.; Scandola, F. *Inorg. Chem.* **1986**, *25*, 4457.

(4) (a) Endicott, J. F.; Ramasami, T. *J. Phys. Chem.* **1986**, *90*, 3740, and articles cited therein. (b) Mayo, S. L.; Ellis, W. R., Jr.; Crutchley, R. J.; Gray, H. B. *Science* **1986**, *233*, 948, and articles cited therein.

(5) (a) Nielson, R. M.; McManis, G. E.; Golovin, M. N.; Weaver, M. J. *J. Phys. Chem.* **1988**, *92*, 3441. (b) Nielson, R. M.; McManis, G. E.; Safford, L. K.; Weaver, M. J. *J. Phys. Chem.* **1989**, *93*, 2152. (c) Nielson, R. M.; McManis, G. E.; Weaver, M. J. *J. Phys. Chem.* **1989**, *93*, 4703.

(6) (a) Weaver, M. J.; Gennett, T. *Chem. Phys. Lett.* **1985**, *113*, 213. (b) Gennett, T.; Milner, D. F.; Weaver, M. J. *J. Phys. Chem.* **1985**, *89*, 2787. (c) McManis, G. E.; Golovin, M. N.; Weaver, M. J. *J. Phys. Chem.* **1986**, *90*, 6563. (d) Nielson, R. M.; Weaver, M. J. *Organometallics*, in press.

(7) Nielson, R. M.; Golovin, M. N.; McManis, G. E.; Weaver, M. J. *J. Am. Chem. Soc.* **1988**, *110*, 1745.

(8) McManis, G. E.; Nielson, R. M.; Weaver, M. J. *Inorg. Chem.* **1988**, *27*, 1827.

0002-7863/89/1511-5533$01.50/0

Generally speaking, the magnitude of H_{12} for a particular internuclear configuration (i.e., precursor complex geometry) can affect the rate constant for that geometry, k_{et} (s^{-1}), by influencing the electronic transmission coefficient, κ_{el}, and additionally the free energy barrier, ΔG^*, as in the conventional expression[1b]

$$k_{et} = \kappa_{el}\nu_n \exp(-\Delta G^*/RT) \quad (1)$$

where ν_n is the nuclear frequency factor. The ν_n term describes the *net* dynamics along the nuclear reaction coordinate in the vicinity of the barrier top, which may include contributions from both collective solvent and inner-shell motion. If only a narrow range of precursor geometries contributes to the bimolecular reaction (vide infra), k_{et} can be related simply to k_{ex} by

$$k_{ex} = K_p k_{et} \quad (2)$$

where K_p is the statistical probability of forming the precursor geometry.[1b,10] If H_{12} is very small, the reaction will be nonadiabatic such that $\kappa_{el} \ll 1$ and $k_{ex} \propto H_{12}^2$ (ref 1b, 2). In the adiabatic regime where H_{12} is sufficiently large so that $\kappa_{el} \rightarrow 1$, the dependence of k_{et} (and hence k_{ex}) upon H_{12} will be milder, arising primarily from the diminution in the barrier height. Evidence from both experimental[1c,3,4a] and theoretical[2] sources suggests that bimolecular reactions, even involving small inorganic reactants, are often nonadiabatic in nature.

While estimates of κ_{el} and hence H_{12} could in principle be obtained from k_{ex} measurements for a single system by using eq 1 and 2, uncertainties in the required estimates of ΔG^* and K_p make this procedure of little utility. One approach is to examine the relative k_{ex} values for a series of structurally related reactions chosen so that differences in the extent of electronic coupling provide a likely major contribution to the observed rate variations.[4a,7] However, due to the involved dependence of κ_{el} upon H_{12} this procedure requires at least an estimate of k_{ex} when $\kappa_{el} \rightarrow 1$ (vide infra).

An attractive, yet virtually unexplored, possibility is to examine additionally the sensitivity of k_{ex} to variations in the nuclear frequency factor ν_n. This is because the dependence of k_{ex} upon ν_n will be sensitive to the degree of reaction nonadiabaticity, which in turn is influenced by the magnitudes both of ν_n and of H_{12}.[11,12] Thus while we expect that $k_{ex} \propto \nu_n$ under adiabatic conditions (i.e., when $\kappa_{el} \sim 1$, eq 1), increasing ν_n for a given H_{12} eventually can lead to a nonadiabatic condition whereupon k_{ex} becomes *independent* of ν_n, since then $\kappa_{el} \propto \nu_n^{-1}$.[11] The form of the k_{ex}–ν_n dependence should therefore be sensitive to, and therefore diagnostic of, the magnitude of H_{12}.[11] While ν_n for processes featuring large inner-shell distortions will be determined at least partly by reactant vibrations that cannot be varied readily, the dynamics of collective solvent motion can provide the dominant contribution to ν_n when the inner-shell barrier is small (say $\lesssim$1 kcal mol^{-1}).[13-15] Substantial (up to 20–50-fold) variations in ν_n can readily be induced under the latter conditions by judicious alterations in the solvent medium, since in many cases $\nu_n \propto \tau_L^{-1}$, where τ_L is the longitudinal solvent relaxation time.[5a,6a-c,13,14] This enables the dependence of k_{ex} upon ν_n to be examined provided that the rates are corrected for the corresponding variations in ΔG^* [5,6] (vide infra).

In the present paper, we exploit such a solvent-dependent analysis to obtain H_{12} estimates for a series of six ferrocene and cobaltocene self-exchange reactions. The k_{ex} values were obtained by using the proton NMR line-broadening technique, with the required solvent dependence of ΔG^* being extracted from optical electron-transfer energies for a related binuclear system, biferrocenylacetylene cation (cf. ref 5). Some of the data used in the present analysis have been discussed previously in a related context.[5] However, the acquisition of additional kinetic and optical barrier data along with our recent reevaluation of the solvent-dependent kinetics for ferrocenium–ferrocene self-exchange[5b] enables the role of orbital overlap in electron transfer to be addressed here quantitatively for the first time. Besides the parent metallocene couples $Cp_2Fe^{+/0}$ and $Cp_2Co^{+/0}$ and the decamethyl derivatives $Cp'_2Fe^{+/0}$ and $Cp'_2Co^{+/0}$, we utilize new solvent-dependent rate data for the (carboxymethyl)cobaltocenium–(carboxymethyl)cobaltocene and (hydroxymethyl)ferrocenium–(hydroxymethyl)ferrocene couples, $(CpCO_2Me)_2Co^{+/0}$ and $(Cp\cdot CpCH_2OH)Fe^{+/0}$, respectively,[5c] abbreviated here as $Cp^e_2Co^{+/0}$ (e = ester) and $HMFc^{+/0}$. These latter two systems were selected initially in view of their water solubility, enabling barrier-crossing dynamics in aqueous and nonaqueous media to be compared.[5c] Together, these six reactant systems are shown here to span a wide (ca. 10-fold) range in H_{12}, from ca. 0.1 to 1.0 kcal mol^{-1}.

Experimental Section

(Carboxymethyl)cobaltocenium tetrafluoroborate was synthesized by stirring the corresponding carboxylic acid derivative $(CpCOOH)_2Co\cdot BF_4$, prepared as in ref 16, in methanol purged with anhydrous HCl for 24 h. Addition of HBF_4 and evaporating some solvent precipitated the desired product, which was recrystallized from hot methanol. The reduced species, (carboxymethyl)cobaltocene, was prepared by stirring a hexane suspension of the salt with a deficiency of cobaltocene. The solution was filtered to remove $Cp_2Co\cdot BF_4$, and the filtrate evaporated to dryness under vacuum. (Hydroxymethyl)ferrocene was synthesized from (trimethylamino)ferrocene (Aldrich) as described in ref 17. The oxidized form, $(Cp\cdot CpCH_2OH)Fe\cdot PF_6$, was prepared by shaking a hexane solution of the reduced species with an acidic aqueous solution containing a 2-fold excess of $FeCl_3$ until the hexane phase became colorless. After filtering, a solution of NH_4PF_6 was added to the aqueous phase to precipitate the desired product. Biferrocenylacetylene (BFA) was prepared as described in ref 18; the acetylferrocene precursor was obtained by acetylation of ferrocene as outlined in ref 19. For all complexes, identification and purity were confirmed by proton NMR and cyclic voltammetry.

The near-infrared spectra, so to obtain optical electron-transfer energies for biferrocenylacetylene cation (BFA^+),[20-22] were measured between 800 and 2000 nm with a Cary Model 17D spectrophotometer, using 1-cm quartz cells. Typically, ca. 1 mM concentrations were employed so to yield maximum absorbances of about 0.2–0.5. For most solvents, BFA^+ was generated from BFA by in situ oxidation with 1 equiv of $Fe(bpy)_3(PF_6)_3$ (bpy = 2,2′-bypyridyl). In some cases (e.g., methanol), the solid $BFA^+BF_4^-$ salt was employed. This was isolated by oxidizing BFA in nitromethane under nitrogen with a stoichiometric quantity of $AgBF_4$ (Aldrich). After filtering, the product was isolated by adding diethyl ether.

Most details of the NMR sample preparation measurements and line-broadening data analysis are given in ref 5a,b. Solvents were high-purity grades from Burdick and Jackson, Aldrich, or Fluka and were purified where appropriate by using standard procedures. Deuterated solvents were employed whenever feasible. However, proteated media were also used successfully by suppressing the solvent peak(s) by using homonuclear irradiation at the desired resonance fequencies, with a minimum of radio-frequency power to avoid significant dielectric heating.[5a] Proton NMR spectra for the $HMFc^{+/0}$ and $Cp^e_2Co^{+/0}$ systems were collected on Nicolet NT 200 and NT 470 instruments, respectively (operated at 200.0 and 469.5 MHz). Due to peak splitting on the Cp ring protons, the line-broadening measurements for these two couples utilized the $-CH_2-$ and methyl substituent proton resonances, respectively. A complication for the former is that the methylene resonance appears as a doublet in the pure diamagnetic species (i.e., hexamethylferrocene) due to spin–spin coupling with the hydroxyl proton. This

(9) Newton, M., personal communication.
(10) Hupp, J. T.; Weaver, M. J. *J. Electroanal. Chem.* **1983**, *152*, 1.
(11) (a) McManis, G. E.; Mishra, A. K.; Weaver, M. J. *J. Chem. Phys.* **1987**, *86*, 5550. (b) Gochev, A.; McManis, G. E.; Weaver, M. J. *J. Chem. Phys.* **1989**, *91*, 906.
(12) (a) Beretan, D. N.; Onuchic, J. N. *J. Chem. Phys.* **1988**, *89*, 6195. (b) Onuchic, J. N.; Beretan, D. N. *J. Phys. Chem.* **1988**, *92*, 4818.
(13) Zusman, L. D. *Chem. Phys.* **1980**, *49*, 295.
(14) Calef, D. F.; Wolynes, P. G. *J. Phys. Chem.* **1983**, *87*, 3387.
(15) (a) Sumi, H.; Marcus, R. A. *J. Chem. Phys.* **1986**, *84*, 4894. (b) Nadler, W.; Marcus, R. A. *J. Chem. Phys.* **1987**, *86*, 3906.
(16) Sheats, J. E.; Miller, W.; Kirsch, T. *J. Organomet. Chem.* **1975**, *91*, 97.
(17) Lindsay, J. K.; Hauser, C. R. *J. Org. Chem.* **1957**, *22*, 355.
(18) Rosenblum, M.; Brawn, N.; Papenmeier, J.; Applebaum, M. *J. Organomet. Chem.* **1966**, *6*, 173.
(19) Graham, R. J.; Lindsey, R. V.; Parshall, G. W.; Peterson, M. L.; Whitman, G. M. *J. Am. Chem. Soc.* **1957**, *79*, 3416.
(20) Powers, M. J.; Meyer, T. J. *J. Am. Chem. Soc.* **1978**, *100*, 4393.
(21) (a) Blackbourn, R. L.; Hupp, J. T. *Chem. Phys. Lett.* **1988**, *150*, 399. (b) Blackbourn, R. L.; Hupp, J. T. *J. Phys. Chem.*, in press.
(22) McManis, G. E.; Gochev, A.; Nielson, R. M.; Weaver, M. J. *J. Phys. Chem.*, in press.

Table I. Summary of Rate Constants, k_{ex}, for Metallocene Self-Exchange Reactions at 25 °C and Related Solvent-Dependent Data

			$10^{-7}k_{ex}$, M^{-1} s^{-1} [d]					
solvent[a]	$10^{-12}\tau_L^{-1}$,[b] s^{-1}	ΔG^*_c,[c]	$Cp'_2Co^{+/0}$ [e]	$Cp^e_2Co^{+/0}$ [f]	$Cp_2Co^{+/0}$ [g]	$Cp'_2Fe^{+/0}$ [h]	$Cp_2Fe^{+/0}$ [h]	$HMFc^{+/0}$ [f]
1. acetonitrile	4[i,j]	5.35	55	20	4.5	3.5	0.9	0.55
2. propionitrile	~4[j,k]	5.15			5.5	3.1	0.92	~0.9
3. acetone	3.5[k]	5.4	28	12	2.3	2.2	0.8	0.72
4. D_2O	1.9[l]	5.2		≈30				1.4
5. nitromethane	4.5[m]	5.3		24		3.7	1.2	~1.4
6. DMF	0.77[n]	(5.0)	25		3.2			
7. DMSO	0.5[o]	(4.9)	23		3.0		0.95	
8. benzonitrile	0.2[p]	4.55	30	8	7.5	6	2.7	1.8
9. nitrobenzene	0.2[p]	4.55		≈4.5		6	3.0	1.4
10. TMU	0.17[q]	(4.85)		4.9	1.55			
11. HMPA	0.11[n]	(4.95)	4.3		0.67			
12. PC	(0.4)[r]	5.25	35	14	3.6		1.2	
13. NMF	0.27[n]	(5.15)			8.5			
14. methanol	(0.135)[s]	5.2		~15	9		1.8	1.7
15. ethanol	(0.033)[t]	5.0			6			

[a] DMF = *N*,*N*-dimethylformamide, DMSO = dimethyl sulfoxide, PC = propylene carbonate, NMF = *N*-methylformamide, TMU = tetramethylurea, HMPA = hexamethylphosphoramide. [b] Inverse of longitudinal solvent relaxation time, obtained from eq 3 by using values of τ_D and ϵ_∞ given in literature values cited, and ϵ_0 either from these sources or ref 23. (In most cases, these values coincide with tabulations in ref 5a and 6c. Where dielectric values not listed in ref 5a or 6c are employed to estimate τ_L, these are given following appropriate footnote to literature citation.) [c] Free energy barrier (in "cusp limit", $H_{12} \to 0$) for self-exchange reactions in a given solvent, estimated from energy of intervalence band maximum, E_{op}, in near-infrared spectra for biferrocenylacetylene cation by using eq 4. Value for D_2O estimated from corresponding E_{op} value for biferrocene cation (see ref 5c). Values in parentheses were estimated as described in the text. [d] Self-exchange rate constant of various cobalt and iron metallocene redox couples in solvent indicated, as obtained by proton NMR line broadening. Cp = cyclopentadienyl, Cp′ = pentamethylcyclopentadienyl, Cp^e = mono(carboxymethyl)cyclopentadienyl, HMFc = hydroxymethylferrocene. All values measured at (or extrapolated to) total ionic strengths $\mu \approx 0.01$–0.02 M. (See ref 5b for details of ionic-strength dependence of k_{ex}.) Reproducibility of k_{ex} values typically within ca. 5–10%, except for $Cp^e_2Co^{+/0}$, for which reproducibility was mostly within ca 20% (see text). [e] Values taken from data in ref 5a but increased by ca. 25% so to account for decrease of μ from 0.14 to 0.02 M. [f] Obtained in present study (also ref 5c). [g] As for footnote *e*, but k_{ex} values in propionitrile and ethanol obtained in present study. [h] Obtained in present study and from ref 5b. [i] Estimated from data in ref 24. [j] Effective τ_L value, estimated by accounting for minor non-Debye characteristics of dielectric loss spectra, appearing as additional loss components at frequencies above τ_D^{-1} (also see ref 25). [k] Estimated from data in ref 26 (also see ref 25). [l] Reference 27. [m] Reference 28. [n] Reference 29. [o] Reference 30 (τ_D = 19 ps, ϵ_∞ = 5.1, ϵ_0 = 46.7). [p] Reference 31. [q] Reference 32. [r] Reference 33. [s] References 34 and 35. [t] Reference 34.

difficulty, however, was circumvented by collapsing the doublet to a single peak by saturating the –OH resonance during NMR data acquisition. In any case, essentially equivalent line widths were obtained irrespective of –OH peak saturation, presumably due to weak CH_2–OH coupling. A difficulty faced with $Cp^e_2Co^{+/0}$ is that the contact shift for the methyl protons is relatively small even at 470-MHz field, ca. 12 ppm, which combined with the relatively large k_{ex} values yields relatively small electron-exchange line broadening. Consequently, it was advisable to correct the measured line widths for magnetic field inhomogeneity. For nonaqueous solvents, this was achieved simply by subtracting the corresponding measured line width for the tetramethylsilane reference signal; the correction was estimated to be 1–2 Hz in D_2O. This complication increases the uncertainties in the derived k_{ex} values for the $Cp^e_2Co^{+/0}$ couple, but they are still probably reliable to within ±20–30%. For the other systems, k_{ex} is typically reproducible to 10–20%.[5] Experimental NMR parameters for the additional reactions studied here are summarized in the supplementary material (see paragraph at the end of the paper).

Results and Discussion

A summary of the k_{ex} values used in the present analysis, for 6 redox couples in 15 solvents, is given in Table I. Besides the additional data gathered in the present work, this summary contains pertinent data culled from ref 5a–c (see footnote to Table I for specific details). For convenience, the k_{ex} values in Table I refer to a uniformly low ionic strength ($\mu \approx 0.01$–0.02 M). This entailed adjusting the values for $Cp'_2Co^{+/0}$ and $Cp_2Co^{+/0}$ given in ref 5a, since these were obtained at $\mu \approx 0.14$ M. Fortunately, this correction is small (ca. 25% in k_{ex}) since k_{ex} for these metallocene couples are insensitive to variations in ionic strength, at least when "noncoordinating" anions (such as PF_6^-, BF_4^-) are employed.[5b] Kinetic data in dichloromethane and dichloroethane, reported in ref 5a, are not included here. This is partly in view of our subsequent observation of deviations from second-order kinetics in these solvents, probably associated with complications from ion pairing. Large ion-pairing effects upon the reaction energetics in such weakly polar media are also evident in optical electron-transfer data.[21a] The k_{ex} values for $Cp_2Fe^{+/0}$, taken in part from ref 5b, differ substantially (up to ca. 10-fold) from those reported by Wahl et al.,[36] which were utilized in our earlier solvent dynamical analyses.[5a,6b] The origins of the systematic solvent-dependent errors in these older data are discussed in ref 5b. Experimental difficulties, such as reactant solubility and decomposition, along with solvent interferences and signal-to-noise constraints in the NMR line-broadening measurements, precluded the evaluation of k_{ex} for a number of redox couple/solvent combinations. For example, the ferrocene couples could not be examined in amide solvents due to decomposition. Nevertheless, sufficient kinetic, along with optical electron transfer (vide infra), data have now been assembled to enable a more sophisticated dynamical analysis than that in ref 5a to be undertaken.

Of the 15 solvents in Table I, the first 11 are considered to approximate "Debye" dynamical behavior in that the dielectric loss spectra can be described in terms of a single relaxation time, τ_D.[37] In this case, the adiabatic barrier-crossing frequency ν_n for electron-transfer reactions having little or no inner-shell barrier is anticipated to be determined by the longitudinal relaxation

(23) Riddick, J. A.; Bunger, W. B. *Organic Solvents*; Wiley-Interscience: New York, 1970.
(24) Arnold, K. E.; Yarwood, J.; Price, A. H. *Mol. Phys.* **1983**, *48*, 452.
(25) McManis, G. E.; Weaver, M. J. *J. Chem. Phys.* **1989**, *90*, 912.
(26) Eloranta, J. K.; Kadaba, P. K. *Trans. Faraday Soc.* **1970**, *66*, 817.
(27) Grant, E. H.; Shack, R. *Trans. Faraday Soc.* **1969**, *65*, 1519.
(28) Nath, D.; Chandra, S. *J. Chem. Phys.* **1969**, *51*, 5299.
(29) Behret, H.; Schmithals, F.; Barthal, J. *Z. Phys. Chem.* **1975**, *96*, 73
(30) Elie, V. *Bull. Soc. Chim. Belg.* **1984**, *93*, 839.
(31) (a) Poley, J. P. *Appl. Sci. Res. B.* **1955**, *4*, 337. (b) Guillaume, F.; Yarwood, J.; Price, A. H. *Mol. Phys.* **1987**, *62*, 1307.
(32) Gaumann, T. *Helv. Chim. Acta* **1958**, *41*, 1956.
(33) Cavell, E. A. S. *J. Chem. Soc., Faraday Trans 2* **1974**, *70*, 78.
(34) (a) Saxton, J. A.; Bond, R. A.; Coats, G. T.; Dickinson, R. M. *J. Chem. Phys.* **1962**, *37*, 2132. (b) Lane, J. A.; Saxton, J. A. *Proc. R. Soc. A* **1952**, *213*, 400.
(35) Barbenza, G. H. *J. Chim. Phys.* **1968**, *65*, 906.
(36) Yang, E. S.; Chan, M.-S.; Wahl, A. C. *J. Phys. Chem.* **1980**, *84*, 3094.
(37) Useful discussions are contained in: (a) Debye, P. *Polar Molecules*; Dover: New York, 1945. (b) *Dielectric Properties and Molecular Behavior*; Hill, N. E., Vaughan, W. E., Price, A. H., Davis, M., Eds.; Van Nostrand Reinhold: London, 1969; Chapters 1 and 5. (c) Smyth, C. P. *Dielectric Behavior and Structure*; McGraw-Hill: New York, 1955. (d) Böttcher, C. J. F.; Bordewyk, P. *Theory of Electric Polarization*; Elsevier: Amsterdam, 1978. (e) For a shorter summary, see: Pottel, R. *Ber. Bunsenges. Phys. Chem.* **1971**, *75*, 286.

time,[13,14] given approximately by[38,39]

$$\tau_L \simeq (\epsilon_\infty/\epsilon_0)\tau_D \quad (3)$$

where ϵ_∞ and ϵ_0 are the "infinite-" and zero-frequency solvent dielectric constants, respectively. The τ_L^{-1} values for each of these solvents are given in Table I (see footnotes and ref 5a and 6c for data sources); the Debye solvents are listed in order of increasing τ_L. Rate data obtained in three noticeably "non-Debye" solvents—propylene carbonate, methanol, and ethanol—are also included in this compilation, along with τ_L^{-1} estimates for the major (low-frequency) relaxation, given in parentheses. (Such non-Debye behavior is characterized by at least one higher-frequency dispersion region having markedly dissipative characteristics.[25,33-35,37]) Although the connection between the dielectric loss spectra and ν_n is considerably less straightforward for non-Debye solvents,[5a,25,40] these kinetic data are nevertheless of interest to the present discussion (vide infra).

As already noted, the central thrust of the present work is to examine the sensitivity of the barrier-crossing frequency to alterations in the solvent dynamics as a means of probing the orbital-overlap factor, H_{12}. Even though only relative, rather than absolute, preexponential factors for a given reaction in a suitable series of solvents are required for this analysis, the solvent-dependent k_{ex} values still need to be corrected for differences in the barrier height, ΔG^*. The required solvent-dependent ΔG^* estimates can be obtained in two ways. The first involves employing theoretical models, most simply the dielectric continuum treatment of Marcus.[41] We have used this approach in several previous discussions.[5a,6a-c]

An alternative, and probably more reliable, procedure utilizes experimental energies for optical electron transfer, E_{op}, within symmetrical mixed-valence compounds that are structurally similar to the thermal electron-exchange reactants of interest.[5] While suitable mixed-valence systems are not abundant, the biferrocenylacetylene cation (BFA^+) constitutes an almost ideal choice for the present purposes. Besides being structurally closely similar to the reactants of interest here, the juxtaposition of the Cp_2Fe^+/Cp_2Fe partners in the binuclear complex[20] roughly mimics that anticipated for the precursor complex for the thermal self-exchange reactions. Most importantly, BFA^+ conforms approximately to "class II" (i.e., valence-trapped) behavior,[20,42] enabling solvent-dependent thermal barriers, ΔG^*_c, to be obtained simply from[1a]

$$\Delta G^*_c = E_{op}/4 \quad (4)$$

It should be noted that ΔG^*_c obtained in this manner is a "cusp" barrier, i.e., in the absence of barrier-top roundedness induced by donor–acceptor orbital overlap ($H_{12} \rightarrow 0$).[1a,43] The actual barriers, ΔG^*, for the present thermal reactions will depend upon the internuclear configuration as well as the metallocene electronic structure (vide infra). However, at least the *solvent dependence* of ΔG^* for a given reaction, as required for the present analysis, should follow approximately the corresponding variations in ΔG^*_c.

The ΔG^*_c estimates obtained from the experimental E_{op} values for BFA^+ in each solvent are also listed in Table I. Values of E_{op} for six of these solvents were reported earlier;[20] the present values agree uniformly within the experimental uncertainty (2–3%). Although substantial ion-pairing effects upon E_{op} have been observed for BFA^+,[21] these effects are small or negligible at the low anion concentrations ($\lesssim$5 mM) and relatively polar media employed for the present E_{op} measurements.[21b] (A brief comparison between the ionic strength dependence of k_{ex} and E_{op} is provided in ref 5b.) The ΔG^*_c value given for D_2O was estimated from E_{op} data for the biferrocene cation, as described in ref 5c, in view of the insolubility of BFA^+ in this solvent. Values of E_{op} could not be obtained for five solvents of interest here (dimethyl sulfoxide and the amides) due to BFA^+ decomposition. Estimates of ΔG^*_c are nevertheless given in parentheses in Table I. These were obtained by taking advantage of the approximate correlation between E_{op} and $(\epsilon_{op}^{-1} - \epsilon_0^{-1})$, where ϵ_{op} is the solvent optical dielectric constant.[20,22] Although there are significant deviations from the *direct proportionality* between E_{op} and $(\epsilon_{op}^{-1} - \epsilon_0^{-1})$ predicted from the dielectric continuum model,[22] the E_{op} values estimated in this manner are likely reliable to within at least $\pm$0.2 kcal mol^{-1}. (The significance of such comparisons to the issue of noncontinuum solvent effects upon ΔG^*_c will be addressed elsewhere.[22]) For simplicity, these ΔG^*_c values are utilized for each redox couple considered here. Slightly (up to 25% smaller) values are anticipated for the decamethyl derivatives in view of their larger size on the basis of the usual continuum treatment.[41] However, given that only the *solvent dependence* of ΔG^*_c is important for the present purposes and that the span of values in Table I is relatively small (<0.9 kcal mol^{-1}), such corrections exert only a small or negligible influence upon the data analysis. In any case, they are of marginal validity, especially given the uncertainties in the precise precursor geometries that contribute to k_{ex} (vide infra).

Rate–Solvent Friction Dependencies. In our previous analyses of solvent dynamical effects for metallocene self-exchange reactions,[5] we obtained solvent-dependent barrier-crossing frequencies, $\kappa_{el}\nu_n$, by inserting the experimental rate constants into eq 1 and 2 together with the corresponding ΔG^* values and a suitable estimate of K_p. The manner and extent of the solvent dynamical influence upon k_{ex} can then be ascertained by examining the dependence of these inferred $\kappa_{el}\nu_n$ values upon known dynamical parameters, most simply τ_L^{-1}.[5]

A somewhat different analysis is employed here. While this simple procedure is desirable for some purposes, as noted above the present objective hinges on examining the functional sensitivity of the net barrier-crossing dynamics to the solvent friction, as reflected in τ_L^{-1}. A complication in employing the preequilibrium treatment (eq 2) for this purpose is that the effective K_p value for a given reaction will tend to vary somewhat with the friction rather than remain constant as is assumed in this analysis.[11b] This is because the distribution of precursor-complex geometries, most simply the range of donor–acceptor spatial separations (r), contributing significantly to the bimolecular reaction rate will inexorably alter as the barrier-crossing dynamics and hence degree of reaction adiabaticity changes.[11b,12] Strictly speaking, the bimolecular rate constant, k_{ex}, even for a pair of "ideal" spherical reactants is composed of an integral of "local" unimolecular rate constants, $k_{et}(r)$, expressed as[44]

$$k_{ex} = (4\pi N/10^3)\int_{r_0}^{\infty} r^2 k_{et}(r)\, g_{DA}(r)\, dr \quad (5)$$

where N is Avogadro's number, r_0 is the donor–acceptor distance corresponding to the reactant's closest approach, and $g_{DA}(r)$ is the radial pair distribution function. [For simplicity, $g_{DA}(r)$ will be taken here as unity.] The radial dependence of k_{et}, and hence

(38) For useful discussions of the relation between τ_L and τ_D, see: (a) Friedman, H. L. *J. Chem. Soc., Faraday Trans. 2* **1983**, *79*, 1465. (b) Hubbard, J.; Onsager, L. *J. Chem. Phys.* **1977**, *67*, 4850. (c) Van der Zwan, G.; Hynes, J. T. *J. Chem. Phys.* **1982**, *76*, 2993. (d) Frolich, H. *Theory of Dielectrics*; Oxford University Press, London, 1949; pp 72–73.

(39) (a) The use of τ_L in such solvent dynamical analyses is subject to some uncertainty due to the accompanying assumption of a dielectric continuum, as well as to uncertainties in the appropriate values of ϵ_∞ to employ in eq 3 (see, for example, ref 25 and the Appendix to ref 11a). However, the inclusion of solvent molecularity effects by using a mean spherical approximation (MSA) yields only small predicted alterations in ν_n.[39b] (b) McManis, G. E.; Weaver, M. J. *J. Chem. Phys.* **1989**, *90*, 1720.

(40) (a) Hynes, J. T. *J. Phys. Chem.* **1986**, *90*, 3701. (b) Sparpaglione, M.; Mukamel, S. *J. Chem. Phys.* **1988**, *88*, 1465, 4300. (c) Rips, I.; Jortner, J. *J. Chem. Phys.* **1987**, *87*, 2090. (d) McManis, G. E.; Weaver, M. J. *Chem. Phys. Lett.* **1988**, *145*, 55.

(41) Marcus, R. A. *J. Chem. Phys.* **1965**, *43*, 679.

(42) In principle, biocobaltocene analogues of BFA^+ could also be examined. However, besides the synthetic difficulties involved, on the basis of a recent comparison between the bicobaltocene and biferrocene cations[8] such species are liable to involve sufficiently strong donor–acceptor orbital overlap so to vitiate the applicability of eq 4.

(43) Hush, N. S. *Electrochim. Acta* **1968**, *13*, 1005.

(44) (a) Tembe, B. L.; Friedman, H. L.; Newton, M. D. *J. Chem. Phys.* **1982**, *76*, 1490. (b) Newton, M. D.; Sutin, N. *Annu. Rev. Phys. Chem.* 1984, *35*, 437.

k_{ex}, is determined primarily by two factors: the diminution in H_{12} (and hence of κ_{el}), and the increases in ΔG^* expected with increasing r. On the basis of eq 1, both of these effects lead to $k_{et}(r)$ decreasing sharply with increasing r. In addition, in the presence of solvent friction ν_n is anticipated to increase significantly with both decreasing H_{12} and increasing ΔG^*, and hence with increasing r.[11,25] All three terms that comprise k_{et} in eq 1 are therefore dependent on the precursor-complex geometry and can therefore influence the k_{ex}–τ_L^{-1} dependence in a relatively complex fashion.[11b]

Although this situation may seem somewhat daunting, these complications may be circumvented in the following manner. Since the ΔG^*_c values in Table I span the narrow range 4.55–5.4 kcal mol^{-1}, the solvent dependence of k_{ex} due to variations in the barrier height may be corrected for by

$$k'_{ex} = k_{ex} \exp[(\Delta G^*_c - 5.0)/RT] \quad (6)$$

where k'_{ex} is the rate constant that would be observed in a given solvent if the cusp-limit barrier was 5.0 kcal mol^{-1}. Since the deviations from this average ΔG^*_c value for the present solvents are less than 0.5 kcal mol^{-1}, the corrections to k_{ex} amount to only 2-fold or less. Although the inevitable uncertainties, perhaps as much as 20–25% (vide supra), in the actual ΔG^*_c values may engender some error in the derived k'_{ex} values,[45] at least the required *relative* k'_{ex} values in the various solvents should be reliable to within 50% or less. The solvent dependence of k'_{ex} will therefore reflect chiefly variations in the preexponential factor caused by alterations in the solvent friction. The nature and extent of this dependence in turn should be sensitive to, and hence diagnostic of, the degree of reaction adiabaticity, and hence H_{12}, for the precursor-complex configurations that contribute most prominently to the observed reaction rates. This procedure is related closely to our previous analysis,[5a] involving the estimation of solvent-dependent $\kappa_{el}\nu_n$ values from the measured rate constants by employing the preequilibrium treatment (eq 1 and 2) and correcting for the barrier height. Such $\kappa_{el}\nu_n$ estimates are instructive for some purposes.[5] However, the spatial integration embodied in eq 5 necessarily considers a range of precursor geometries with spatially dependent preexponential and exponential factors (vide infra). For the present purposes, therefore, it is preferable to explore the solvent-dependent dynamical effects in terms of k'_{ex} rather than to extract ν_n estimates from the rate data.

Plots of log k'_{ex} versus log τ_L^{-1} for 5 metallocene couples in 11 "Debye" solvents, extracted from the k_{ex} and ΔG^*_c values in Table I by using eq 6, are given in Figure 1. The solvent numbering scheme is as listed in Table I; the three filled symbols (circles, squares, and triangles) refer to $Cp'_2Co^{+/0}$, $Cp^e_2Co^{+/0}$, and $Cp_2Co^{+/0}$, respectively, whereas the two open symbols (triangles and squares) refer to $Cp_2Fe^{+/0}$ and $HMFc^{+/0}$, respectively. (The points for $Cp'_2Fe^{+/0}$ are not shown for clarity in Figure 1 since these are uniformly close to the corresponding $Cp_2Co^{+/0}$ points.) Comparably shaped log k'_{ex}–log τ_L^{-1} plots, yet having somewhat larger shapes, are also obtained if the dielectric continuum estimates of ΔG^*_c (as used in ref 5a) are employed instead to estimate k'_{ex} from k_{ex}. As noted above, however, the present experimentally derived values of ΔG^*_c are probably more reliable than such theoretical estimates.

Inspection of Figure 1 reveals that the degree of dependence of log k'_{ex} upon log τ_L^{-1} depends markedly upon the redox couple. For the most facile $Cp'_2Co^{+/0}$ couple, the log k'_{ex}–log τ_L^{-1} slope approaches unity yet appears to decrease as the solvent friction decreases (i.e., for higher τ_L^{-1} values). A similar log k'_{ex}–log τ_L^{-1} dependence is obtained for $Cp^e_2Co^{+/0}$, although the data set is more restricted. The less facile $Cp_2Co^{+/0}$ couple also displays a qualitatively similar dependence of log k'_{ex} upon log τ_L^{-1}; however,

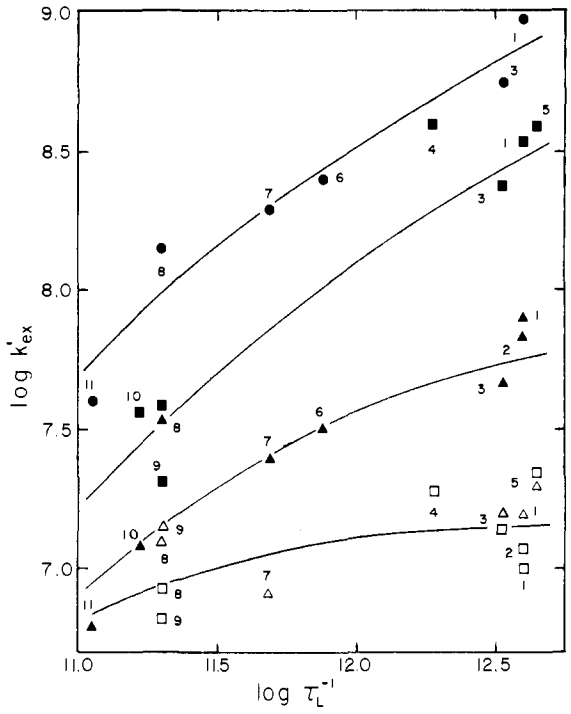

Figure 1. Logarithmic plots of "barrier-corrected" rate constants, k'_{ex}, versus inverse of longitudinal relaxation time, τ_L^{-1}, for 5 metallocene redox couples in 11 solvents. k'_{ex} values were extracted from experimental k_{ex} and ΔG^*_c values given in Table I by using eq 6. See Table I for solvent numbering scheme. Key to redox couples: $Cp'_2Co^{+/0}$, filled circles; $Cp^e_2Co^{+/0}$, filled squares; $Cp_2Co^{+/0}$, filled triangles; $Cp_2Fe^{+/0}$, open triangles; $HMFc^{+/0}$, open squares. Solid traces through each set of solvent-dependent log k'_{ex} values are suggested "best-fit" curves (see text).

the slopes are noticeably smaller (Figure 1). While the k'_{ex} value for $Cp_2Co^{+/0}$ in benzonitrile (point 8) is significantly (ca. 2-fold) larger than expected on this basis, the remaining log k'_{ex}–log τ_L^{-1} correlation is satisfactory, displaying a decidedly fractional slope (ca. 0.3–0.5) toward the highest τ_L^{-1} values. The least facile ferrocene couples $Cp_2Fe^{+/0}$ and $HMFC^{+/0}$ exhibit no clear dependence of log k'_{ex} upon log τ_L^{-1}, even though the absence of rate data for these reactions in amides restricts somewhat the range of solvents.

Consequently, therefore, an interesting spectrum of dynamical behavior is evident. This spans the range from apparently full "solvent dynamical control", where $k'_{ex} \propto \tau_L^{-1}$, for the most facile cobaltocene reactions in relatively high friction (small τ_L^{-1}) media, to largely nonadiabatic behavior ("electron-tunneling control"), reflected in the insensitivity of k'_{ex} to τ_L^{-1} for the least facile ferrocene systems. As outlined below, the combination of such varying rate-friction dependencies for such a "homologous series" of reactions, together with the rate differences between the reactions in a given solvent, enable *absolute* estimates of H_{12} to be obtained. Uncertainties in the data analysis together with other factors limit our confidence in some quantitative details (vide infra). Nevertheless, the solid traces included in Figure 1 represent intuitive "best fits" of the log k'_{ex}–log τ_L^{-1} dependencies for each reaction. (Only one trace is drawn for the $Cp_2Fe^{+/0}$ and $HMFc^{+/0}$ couples in view of their closely similar kinetic behavior.)

These results are displayed in a somewhat different form in Table II, which lists k'_{ex} values ratioed to the corresponding quantity in acetonitrile, k'_{ex}(ACN). (Acetonitrile was chosen as a "reference" solvent here in view of its rapid relaxation behavior together with the availability of reliable k_{ex} values for all six metallocene couples.) Given alongside these k'_{ex}/k'_{ex}(ACN) values are the corresponding τ_L^{-1}/τ_L^{-1}(ACN) ratios, which should approximate the rate ratios only if overdamped solvent dynamical control is maintained. While the k'_{ex}/k'_{ex}(ACN) values for $Cp'_2Co^{+/0}$ and $Cp^e_2Co^{+/0}$ self-exchange in Debye solvents decrease uniformly in parallel with τ_L^{-1}/τ_L^{-1}(ACN), the rate ratios for the

(45) A possible additional limitation of eq 6 is that E_{op} and hence ΔG^*_c refer to a particular precursor complex geometry, whereas in actuality k_{ex} reflects an integral of reaction sites (eq 5) with varying ΔG^* (see eq 8 and 9). However, eq 6 is expected to be valid to a good approximation since the predominant contribution to k_{ex} should usually arise from geometries close to reactant "contact", for which at least the *solvent dependence* of ΔG^* should be close to that for ΔG^*_c.[11b]

Table II. "Barrier-Corrected" Rate Constants for Metallocene Self-Exchange in Various Solvents Relative to those in Acetonitrile, $k'_{ex}/k'_{ex}(ACN)$, in Comparison with Corresponding Relative Solvent Relaxation Dynamics, $\tau_L^{-1}/\tau_L^{-1}(ACN)$

		$k'_{ex}/k'_{ex}(ACN)^c$					
solvent[a]	$\tau^{-1}_L/\tau_L^{-1}(ACN)^b$	$Cp'_2Co^{+/0}$	$Cp^e_2Co^{+/0}$	$Cp_2Co^{+/0}$	$Cp'_2Fe^{+/0}$	$Cp_2Fe^{+/0}$	$HMFc^{+/0}$
propionitrile	~1			0.9	0.65	0.75	1.2
acetone	0.9	0.6	0.7	0.6	0.7	1.0	1.4
D_2O	0.5		1.2				2
nitromethane	≈1.1		1.1		1.0	1.25	2.3
DMF	0.2	0.25	0.13	0.4			
DMSO	0.12	0.2		0.3		0.5	
benzonitrile	0.05	0.15	0.11	0.4	0.45	0.8	0.9
nitrobenzene	0.05		0.06		0.45	0.9	0.7
TMU	0.043		0.11	0.15			
HMPA	0.028	0.04		0.075			
PC	(0.1)	0.55	0.6	0.65			1.9
NMF	0.07			1.4			
methanol	(0.035)		0.6	1.6		1.55	2.4
ethanol	(0.008)			0.75			

[a] See footnote *a* to Table I for explanation of abbreviations. [b] Ratio of inverse longitudinal relaxation time for given solvent to that in acetonitrile. See Table I for τ_L^{-1} values and data sources. [c] Ratio of barrier-corrected rate constant, k'_{ex}, for given metallocene redox couple in various solvents to that in acetonitrile, $k'_{ex}(ACN)$. Values of k'_{ex} obtained from experimental k_{ex} and ΔG^*_c values (Table I) by using eq 6. See footnote *d* of Table I for explanation of metallocene abbreviations.

Table III. Ratios of Rate Constants for Metallocene Self-Exchange to Those of $Cp'_2Co^{+/0}$, $k_{ex}/k_{ex}(Cp'_2Co)$, in Various Solvents

		$k_{ex}/k_{ex}(Cp'_2Co)^c$				
solvent[a]	$10^{-12}\tau_L^{-1}$,[b] s^{-1}	$Cp^e_2Co^{+/0}$	$Cp_2Co^{+/0}$	$Cp'_2Fe^{+/0}$	$Cp_2Fe^{+/0}$	$HMFc^{+/0}$
acetonitrile	4	0.35	0.08	0.065	0.015	0.010
acetone	3.5	0.43	0.08	0.08	0.03	0.025
PC	(0.4)	0.4	0.11			0.035
DMF	0.77		0.13			
DMSO	0.5		0.13			
benzonitrile	0.2	0.27	0.25	0.20	0.09	0.06
HMPA	0.11		0.16			

[a] See footnote *a* to Table I for explanation of abbreviations. [b] Inverse longitudinal solvent relaxation time (as in Table I). [c] Calculated from k_{ex} values in Table I.

other couples in a given solvent are seen to increase in the sequence $Cp'_2Co^{+/0} \sim Cp^e_2Co^{+/0} < Cp_2Co^{+/0} \lesssim Cp'_2Fe^{+/0} < Cp_2Fe^{+/0} \lesssim HMFc^{+/0}$, the dependence becoming more marked as $\tau_L^{-1}/\tau_L^{-1}(ACN)$ decreases (Table II). This finding is consistent with a progressive decrease in the degree of solvent dynamical control for the less facile redox couples, the dependence of k'_{ex} upon τ_L^{-1} being almost entirely absent for $Cp_2Fe^{+/0}$ and $HMFc^{+/0}$ (cf. ref 5b).

Also included in Table II are corresponding data for the three non-Debye solvents propylene carbonate (PC), methanol, and ethanol, along with the strongly hydrogen-bonded liquid *N*-methylformamide (NMF). In accordance with previous discussions,[5a,25] the k'_{ex} values for $Cp^e_2Co^{+/0}$ and $Cp_2Co^{+/0}$ in these solvents are much larger than expected from the corresponding τ_L^{-1} values. By comparing the k'_{ex} values with corresponding values in Debye media so to achieve the best consistency with the other k'_{ex}–τ_L^{-1} data, "effective" inverse relaxation times, τ_{eff}^{-1}, can be deduced in these non-Debye solvents (cf. ref 40d). This procedure yields approximate τ_{eff}^{-1} values as follows: PC, 2×10^{12} s^{-1}; methanol, $\gtrsim 3 \times 10^{12}$ s^{-1}; ethanol, 4×10^{12} s^{-1}; NMF, $> 3 \times 10^{12}$ s^{-1}. These enhanced barrier-crossing frequencies are roughly consistent with some theoretical predictions.[25] They are also in harmony with some very recent information on real-time polar solvation dynamics extracted from subpicosecond fluorescence measurements;[46a] a detailed comparison between τ_{eff} obtained from electron-transfer and time-resolved fluorescence measurements will be featured in a forthcoming article.[46b]

A related illustration of the variations in the degree of electron-tunneling versus solvent-dynamical control as the solvent is altered is provided in Table III, which lists ratios of k_{ex} values for each metallocene versus that for $Cp'_2Co^{+/0}$, $k_{ex}/k_{ex}(Cp'_2Co)$, in seven solvents. The advantage of this format is that no knowledge of the *solvent dependence* of the free-energy barriers is required, since this should largely cancel when the rate ratios are taken. The variations in these ratios with the solvent therefore provide a monitor of the extent to which the *relative* barrier-crossing frequencies for the different reactions are sensitive to the solvent dynamics. To facilitate comparison, the solvents are again listed in order of decreasing τ_L^{-1}, although data in PC are inserted in a position commensurate with the τ_{eff}^{-1} value inferred above, 2×10^{12} s^{-1}. The increasing emergence of electron-tunneling control of k_{ex} as the τ_L^{-1} value is increased or the redox couple is altered in the sequence $Cp'_2Co^{+/0} < Cp^e_2Co^{+/0} < Cp_2Co^{+/0} < Cp'_2Fe^{+/0} < Cp_2Fe^{+/0} < HMFc^{+/0}$ can be discerned clearly in the progressive decreases in the $k_{ex}/k_{ex}(Cp'_2Co)$ ratios observed under these conditions (i.e., up the columns and across the rows, respectively, in Table III).

Extraction of Electronic Coupling Matrix Elements. A relatively direct means of extracting the extent of electronic coupling for each reaction from the results in Figure 1 involves matching them with a corresponding sequence of curves obtained using k'_{ex} values, $k'_{ex}(calcd)$, calculated from a theoretical model for a suitable sequence of H_{12} values. Figure 2 displays such a set of log $k'_{ex}(calcd)$–log τ_L^{-1} curves obtained for the same solvents as in Figure 1. A detailed presentation of the underlying theory forms the subject of ref 11b. (See also the Appendix below.) Briefly, the $k'_{ex}(calcd)$ values in each solvent were calculated by utilizing eq 5 with the spatial integration performed from a distance of closest approach, r_0, of 7.6 Å (i.e., twice the metallocene radius, 3.8 Å[5a]). The dependence of the "local" (unimolecular) rate constant, k_{et}, upon the reactant internuclear separation, r, required in eq 5, was obtained as follows. The primary input parameters are τ_L, H_{12}, and ΔG^*. While τ_L can be considered to be r independent for the present purposes,[39] both H_{12} and ΔG^* are sensitive to the reactant pair geometry.

The r dependence of the former can be taken as[2]

$$(H_{12})^2 = (H^\circ_{12})^2 \exp[-\alpha(r - r_0)] \quad (7)$$

(46) (a) Kahlow, M. A.; Jarzeba, W.; Kang, T. J.; Barbara, P. F. *J. Chem. Phys.* **1989**, *90*, 151, and earlier papers cited therein. (b) Barbara, P. F.; Weaver, M. J., to be published.

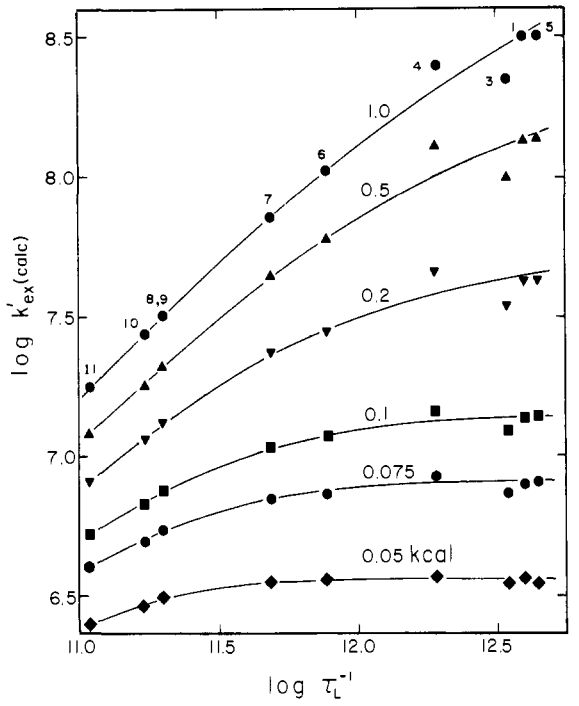

Figure 2. Logarithmic plots of calculated "barrier-corrected" rate constants, k'_{ex}(calcd), versus inverse of longitudinal relaxation time, τ_L^{-1}, in the same 11 solvents as for Figure 1, for the sequence of 6 electronic matrix coupling elements at reactant "contact", H°_{12}, as indicated. Values of k'_{ex}(calcd) obtained from corresponding calculated values, k_{ex}(calcd), in each solvent by using eq 6 in the same manner as for the experimental quantities. Values of k_{ex}(calcd) obtained by using spatial integration procedure (eq 5) with r_0 taken as 7.6 Å and $g_{DA}(r) = 1$. Required values of $k_{et}(r)$ obtained from eq A1 with constituent quantities calculated as follows: k^{TST} from eq A2 using "solvent inertial" frequencies, ω_0, calculated as described in ref 25 (see footnotes to Figure 4 and Table II of ref 25 for numerical values); $k^a_{et}(r)$ from eq 9–16 of ref 11b (also see eq A4 and A5 in the Appendix); $\tilde{\kappa}_{el}$ from eq A6 and A7 (see Appendix). The r-dependent ΔG^* values required for k^{TST} and $k^a_{et}(r)$ were obtained from eq 8 and 9 with $\Delta G^*_c(r_0)$ as given in Table I and $a = 3.8$ Å. The r-dependent H_{12} values also required in eq 8, as well as for calculating $\tilde{\kappa}_{el}$, were obtained from eq 7 with $\alpha = 1.25$ Å^{-1}. The double integrals required using this overall procedure (both spatially and along the reaction coordinate[11b]) were evaluated by using a standard two-dimensional quadrature technique,[64] executed on the Purdue University Cyber 205 supercomputer using double precision (128 bit).

where H°_{12} is the matrix coupling element for the "closest approach" geometry. The coefficient α is taken here to be the typical value 1.25 Å^{-1}.[2,11b] The corresponding r-dependent barrier height is obtained from[11b]

$$\Delta G^* = \Delta G^*_c - H_{12} \quad (8)$$

In addition to the increase in ΔG^* with increasing r due to corresponding decreases in H_{12}, ΔG^*_c and hence ΔG^* should also increase under these conditions according to[11b]

$$\Delta G^*_c(r) = \Delta G^*_c(r_0)[2a(a^{-1} - r^{-1})] \quad (9)$$

where a is the reactant radius and $\Delta G^*_c(r_0)$ is the cusp barrier height when $r = r_0$ ($=2a$). This latter quantity was set equal to the ΔG^*_c values given for each solvent in Table I. Although the radial dependence of ΔG^*_c in eq 9 has its origin in the two-sphere dielectric continuum treatment,[41] it is also approximately consistent with r-dependent E_{op} measurements for biferrocene cations[20] and related systems.[1a,f] Strictly speaking, eq 9 presumes that ΔG^*_c arises entirely from solvent reorganization, i.e., the inner-shell (reactant vibrational distortional) barrier, ΔG^*_{is}, is small. Although our earlier estimates for ΔG^*_{is} for these metallocene couples[6b,7] are marred by a systematic error in the bond-distance estimates, it is likely that $\Delta G^*_{is} \approx 0.5$–1 kcal mol^{-1}.[47] (Note that the E_{op} estimates of ΔG^*_c necessarily contain any inner-shell contribution to the binuclear redox system.)

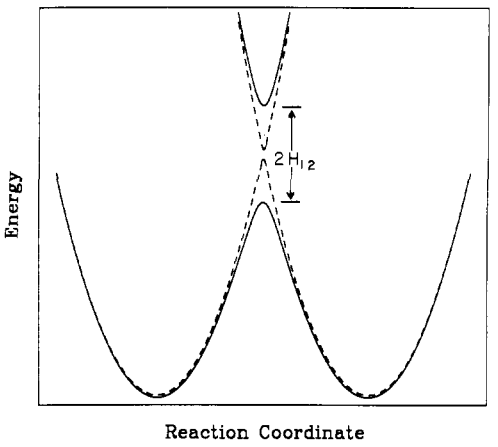

Figure 3. Schematic free energy–reaction coordinate profiles for electron-exchange reactions having different electronic matrix coupling elements, H_{12}. Curves calculated by using eq 4 and 5 of ref 11a. For a 5 kcal mol^{-1} cusp barrier, the solid and dashed traces shown correspond to H_{12} values of 1.0 and 0.1 kcal mol^{-1}, respectively.

In essence, the calculation of $k_{et}(r)$ and hence k'_{ex}(calcd) from these parameters involves evaluating the corresponding adiabatic rate constant $k^a_{et}(r)$, and the corresponding modifications to account for nonadiabatic barrier crossing. The latter was accomplished here by using eq A1 in the Appendix; note that generally $k_{et} \leq k^a_{et}$. These nonadiabatic effects ($\kappa_{el} < 1$) are felt increasingly for smaller H_{12} and/or larger τ_L^{-1}. The calculation of k^a_{et} takes into account the influences of barrier-top roundedness (i.e., nonzero H_{12}) as well as the effect of solvent friction (via τ_L) upon the barrier-crossing frequency ν_n. Equation A1 also includes the effects of solvent inertia; these yield deviations from pure "overdamped" behavior (where $\nu_n \propto \tau_L^{-1}$) anticipated in low-friction media where ν_n approaches the transition-state theory (TST) limit, whereupon ν_n equals the solvent inertial frequency $\omega_0/2\pi$ and $k^a_{et} = k^{TST}$.[6b,14,25] (See Appendix and ref 11b.)

The six sets of points shown in Figure 2, with "best-fit" curves drawn through each set, correspond to the H°_{12} values, from 0.05 to 1.0 kcal mol^{-1}, as indicated. (The particular solvents are identified by the same numbering scheme as in Table I and Figure

(47) The differences in metal–ring bond distance between the reduced and oxidized metallocene forms, Δa, given in ref 6b and 7 were obtained largely from corresponding metal–Cp carbon bond distances, d_{M-C}, as listed in footnote *h* to Table I of ref 6b (with literature sources), along with carbon–ring centroid distances, d_{C-rc}. However, these Δa values are ca. 30–40% smaller than the true estimates due to a trigonometrical error. (We are grateful to Dr. Marshall Newton for bringing this point to our attention.) Employing the relevant d_{M-C} values in the Pythagorean theorem along with the corresponding d_{C-rc} values (1.19–1.20 Å) yields the following revised Δa values: $Cp'_2Co^{+/0}$, 0.065 Å; $Cp_2Co^{+/0}$, ~0.07 Å; $Cp'_2Fe^{+/0}$, ~0.055 Å. (As before,[6b,7] we take Δa for $Cp_2Fe^{+/0}$ to equal that for $Cp'_2Fe^{+/0}$ in lieu of adequate bond-distance data for ferrocene.) Combined with the corresponding reduced force constants, f_r, for the M–Cp stretch for $Cp_2Co^{+/0}$ and $Cp_2Fe^{+/0}$, 4.0×10^5 and 3.75×10^5 dyn cm^{-1}, respectively (footnote 15 of ref 7), we obtain ΔG^*_{is} values of about 1.4 and 0.8 kcal mol^{-1}. (Note that these f_r values refer to the effective force constant for each M–Cp "bond" as the Cp–M–Cp unit undergoes symmetric distortion; these values are equal to the sum of the individual M–Cp force constant and the "interaction force constant" derived from Raman and infrared frequencies.[48,49]) The revised ΔG^*_{is} values are about twice the former estimates[7] but are only very approximate given the lack of more reliable bond-distance data (and the complete absence of solution-phase data) together with the simplified force-constant calculations. A somewhat smaller f_r value, 2.3×10^5 dyn cm^{-1}, is obtained from Raman spectra for $Cp'_2Fe^{+/0}$[50] (footnote 17 of ref 7), yielding $\Delta G^*_{is} \approx 0.5$ kcal mol^{-1}. Although corresponding vibrational data for $Cp'_2Co^{+/0}$ are unavailable, a roughly similar ΔG^*_{is} estimate can be assumed for this couple. However, the apparently smaller effective Cp–M–Cp force constant observed upon methylation of ferrocene is perhaps questionable.[51]

(48) For example: Hartley, D.; Ware, M. J. *J. Chem. Soc. A* **1969**, 138.

(49) Herzberg, G. *Infrared and Raman Spectra of Polyatomic Molecules*; Van Nostrand: New York, 1945; p 187.

(50) Duggan, D. M.; Hendrickson, D. N. *Inorg. Chem.* **1975**, *14*, 955.

(51) Luthi, H. P.; Ammeter, J. H.; Almlöf, J.; Faegri, K., Jr. *J. Chem. Phys.* **1982**, *72*, 2002.

1.) By and large, the calculated curves (Figure 2) show a striking similarity to the corresponding experimental plots in Figure 1, in that the log k'_{ex}(calcd)–log τ_L^{-1} slopes decrease for smaller H°_{12} and/or larger τ_L^{-1}, reflecting increasing reaction nonadiabaticity. Indeed, it is interesting to note that even the scatter in the calculated points in Figure 2 for solvents having the largest τ_L^{-1} values (D_2O, acetone, acetonitrile, and nitromethane) is mimicked reasonably well by the experimental data in Figure 1. (This scatter arises from the onset of an inertial limit upon k_{ex} which is solvent dependent, ω_0 being largest for D_2O and smallest for acetone[25]).

We therefore have reasonable confidence in extracting approximate estimates of H°_{12} for the various experimental systems by matching the shapes of the experimental and calculated log k'_{ex}–log τ_L^{-1} curves, together with the vertical displacement between them. This procedure yields the following H°_{12} estimates (kcal mol^{-1}): $Cp'_2Co^{+/0}$, 1.0; $Cp^e_2Co^{+/0}$, 0.5–1.0; $Cp_2Co^{+/0}$, 0.25; $Cp'_2Fe^{+/0}$, 0.2; $Cp_2Fe^{+/0}$, 0.1; $HMFc^{+/0}$, 0.075. As a pictorial illustration of these differences, Figure 3 shows a pair of free energy reaction coordinate profiles, calculated as in ref 11a, appropriate for ΔG^*_c = 5 kcal mol^{-1} with H_{12} = 1.0 (solid curve) and 0.1 kcal mol^{-1} (dashed curve).

The above H°_{12} estimates for the cobaltocene systems, especially $Cp_2Co^{+/0}$, may well be significantly smaller than the actual values given the possibility that ΔG^*_{is} for these couples, are slightly (ca. 0.5 kcal mol^{-1}) larger than for the ferrocene systems.[47] The presence of such increased ΔG^*_{is} not only will decrease k'_{ex} in a given solvent but also may diminish significantly the influence of solvent friction, i.e., depress the log k'_{ex}–log τ_L^{-1} dependence.[15,52] At least the latter complication, however, should disappear in the dynamically most rapid solvents, where τ_L^{-1} (or $\omega_0/2\pi$) approaches the vibrational frequencies, ca. (6–9) × 10^{12} s^{-1},[6b] characterizing the symmetric Cp–M–Cp inner-shell distortions.[15] If ΔG^*_{is} is indeed 0.5 kcal mol^{-1} larger for $Cp_2Co^{+/0}$ than for $Cp_2Fe^{+/0}$, then to correct for this difference the log k'_{ex} values for the former couple will need to be increased by 0.35 (i.e., ca. 2.5-fold in k'_{ex}) at the largest log τ_L^{-1} values in Figure 1. This would yield a log k'_{ex} difference of 1.0 rather than ca. 0.65 for these couples in, say, acetonitrile and acetone. Assuming that $H^\circ_{12} \approx 0.1$ kcal mol^{-1} for $Cp_2Fe^{+/0}$, it can be deduced from Figure 2 that this correction yields an approximately 2-fold enhancement in the H°_{12} estimate for $Cp_2Co^{+/0}$, from ca. 0.25 to 0.5 kcal mol^{-1}.

The ca. 3-fold larger k'_{ex} values for $Cp'_2Co^{+/0}$ relative to $Cp^e_2Co^{+/0}$ observed in each solvent may also be attributable in part to differences in ΔG^*_{is}.[47] This behavior is also consistent with a smaller outer-shell (solvent reorganization) barrier for the former couple that might be anticipated from its slightly larger effective radius. Alternatively, H°_{12} for $Cp'_2Co^{+/0}$ may be even larger than 1.0 kcal mol^{-1}. Apart from the uncertainties in extracting the solvent-dependent k'_{ex} values themselves, the estimated τ_L values are subject to significant error.[39a] The assumption that the first 11 solvents in Table I exhibit Debye behavior is, of course, only an approximation, even though the most recent subpicosecond time-resolved fluorescence data yield major relaxation times that typically differ from τ_L by 2-fold or less.[39a] [The observed positive deviations of the k'_{ex} values from the anticipated log k'_{ex}–log τ_L^{-1} plots in benzonitrile, for example (Figure 1), may be due to the influence of a higher frequency relaxation in this solvent.] Possible solvent-specific effects upon the approach of the reacting partners, which would be reflected in nonunit $g_{DA}(r)$ values (eq 5), may also contribute significantly to the rate–solvent dependence. Generally speaking, however, consideration of these and related factors lead only to relatively minor (<2-fold) uncertainties in the inferred H°_{12} estimates. The relative H°_{12} values, then, are deemed sufficiently reliable to warrant at least semiquantitative interpretation.

Table IV. Comparison between Self-Exchange Rate Constants for Various Metallocene Redox Couples in Acetonitrile at 25 °C and Corresponding Formal Potentials

redox couple[a]	E_f,[b] V vs $Cp_2Fe^{+/0}$	k_{ex},[c] M^{-1} s^{-1}
$Cp'_2Co^{+/0}$	−1.92	5.5 × 10^8
$Cp_2Co^{+/0}$	−1.30	4.5 × 10^7
$Cp^e_2Co^{+/0}$	−0.79	2.0 × 10^8
$Cp'_2Fe^{+/0}$	−0.50	3.5 × 10^7
$(Cp{\cdot}CpCH_2OH)Fe^{+/0}$	−0.01	5.5 × 10^6
$Cp_2Fe^{+/0}$	0	9 × 10^6
$(Cp{\cdot}CpI)Fe^{+/0}$	0.15	9.2 × 10^6
$(Cp{\cdot}CpCOCH_3)Fe^{+/0}$	0.24	8.0 × 10^6
$(Cp{\cdot}CpCN)Fe^{+/0}$	0.36	5.7 × 10^6

[a] Nomenclature partly as in Tables I–III. [Note that (hydroxymethyl)ferrocenium–(hydroxymethyl)ferrocene is abbreviated as $(Cp{\cdot}Cp{\cdot}CH_2OH)Fe^{+/0}$ rather than $HMFc^{+/0}$ for consistency with other monosubstituted ferrocenes listed here.] [b] Formal potential (volts) versus ferrocenium–ferrocene in same solvent (acetonitrile) evaluated at gold or mercury electrodes in 0.1 M tetrabutylammonium hexafluorophosphate by using cyclic voltammetry. [c] Rate constant for metallocene self-exchange in acetonitrile, for ionic strength $\mu \sim$ 0–0.02 M, taken from Table I and ref 57. Values reproducible generally to ±10–20%.

Interpretation and Implications of H°_{12} Values. The markedly (ca. 2.5–5-fold) larger H°_{12} values estimated for $Cp_2Co^{+/0}$ and other cobaltocene couples compared with their ferrocene analogues can be accounted for in terms of the spatial differences in the "redox molecular orbitals", corresponding to the LUMO/HOMO pair[53] for the Cp_2M^+/Cp_2M reaction partners.[7] While theoretical studies indicate that the cobaltocene HOMO is delocalized over the Cp rings,[54] that for ferrocene is strongly metal centered.[55] Since similar considerations also apply to the LUMO for the oxidized redox forms,[54,55] the donor–acceptor orbital overlap should be greater for the $Cp_2Co^{+/0}$ versus the $Cp_2Fe^{+/0}$ couples.[7] The relative H°_{12} values for these reactions are in harmony with the 2-fold greater H_{12} estimates derived from optical electron-transfer data for bicobaltocene versus biferrocene cations,[8] although the absolute values of the latter are much larger (3.2 and 1.7 kcal mol^{-1}, respectively) partly as a result of direct bond formation between the redox centers.

Very recent ab initio calculations by Newton also yield markedly (ca. 3–6-fold) larger H_{12} values for $Cp_2Co^{+/0}$ than for $Cp_2Fe^{+/0}$ self-exchange.[9] These calculations also indicate that considerably stronger overlap is obtained for approach of the reacting pair along a common 5-fold axis ("axial" geometry) than for a "side-by-side" configuration. For the former geometry, H_{12} = 2.5 and 0.4 kcal mol^{-1} for $Cp_2Co^{+/0}$ and $Cp_2Fe^{+/0}$, respectively, when the Cp rings are "in contact" (3.5 Å apart); whereas in the latter configuration, $H^\circ_{12} \approx$ 0.04 and 0.1 kcal mol^{-1}, respectively.[9] These findings foreshadow a limitation in the present analysis; the substantial anisotropy in the calculated H_{12} values suggests that the assumption of spherical symmetry embodied in eq 5 is, strictly speaking, inadequate. Nevertheless, the present experimental H°_{12} estimates should represent at least weighted averages of the true values for the various "close contact" encounter pair geometries and as such are reasonably consistent with the calculated values. It would be of interest to perform more sophisticated kinetic

(52) This effect arises since in the presence of a significant reactant distortional component, barrier passage can take place via vibrational relaxation from a significant distribution of solvent polarization states.[15] The presence of such an additional "vibrational reaction coordinate" will thereby enhance ν_n to an extent that increases with increasing solvent friction (i.e., as the effective frequency characterizing solvent relaxation, τ_L^{-1}, decreases). Consequently, the k_{ex}–τ_L^{-1} slopes should be smaller in the presence of such vibrational relaxation, to an extent that depends on its relative contribution to the effective barrier.

(53) (a) LUMO = lowest unoccupied molecular orbital; HOMO = highest occupied molecular orbital. (b) Note that consideration of *molecular* orbitals derived from a basis set that includes the ligand as well as the metal center can account for so-called electron "superexchange" mechanisms which utilize predominantly ligand orbital overlap.[2d]

(54) (a) Weber, J.; Goursot, Penigault, E.; Ammeter, J. H.; Bachmann, J. *J. Am. Chem. Soc.* **1982**, *104*, 1491. (b) Famighetti, C.; Baerends, E. J. *Chem. Phys.* **1981**, *62*, 407.

(55) (a) Zerner, M. C.; Loew, G. H.; Kirchner, R. F.; Mueller-Westerhoff, U. T. *J. Am. Chem. Soc.* **1980**, *102*, 589. (b) Bagus, P. S.; Wahlgren, U. I.; Almlöf, J. *J. Chem. Phys.* **1976**, *64*, 2324. (c) Rosch, N.; Johnson, K. H. *Chem. Phys. Lett.* **1974**, *24*, 179.

(56) For example: Gordon, A. J.; Ford, R. A. *The Chemist's Companion*; Wiley-Interscience: New York, 1972; p 146.

(57) Nielson, R. M., unpublished observations.

analyses employing such detailed theoretical information.

Interpretation of the substantial observed variation in H°_{12} resulting from Cp ring substitution, unlike alteration of the metal center, is limited by the lack of electronic structural information for these systems. At first sight, one might expect that H°_{12} would correlate roughly with empirical electronic quantities such as the Hammett σ parameter, which characterizes substituent effects in organic chemistry,[58] especially since they correlate well with metallocene formal potentials[59,60] and NMR chemical shifts.[61]

To this end, Table IV contains k_{ex} values in acetonitrile for the self-exchange reactions studied here, together with some additional data for four monosubstituted ferrocenes,[57] in comparison with corresponding formal potentials, E_f. (The entries are listed in order of increasing E_f.) As noted above, the differences in k_{ex} in this dynamically rapid solvent should be particularly sensitive to variations in H_{12}. The lack of any correlation between k_{ex} and E_f for either the cobaltocene and ferrocene couples is evident, even though substantial variations in both these quantities are observed. Upon reflection, however, this finding is unsurprising since the substituent effect upon E_f arises from alterations in the *energy* of the redox orbital. Although orbital energetics can influence H_{12} via superexchange mechanisms,[53b] H_{12} and hence k_{ex} should be responsive additionally to the *spatial* properties of the HOMO/LUMO pair.[62] Given the magnitude of such apparent substituent effects upon H_{12}, their further detailed examination would be of great interest.

As noted previously,[7] the sensitivity of the self-exchange kinetics to the metallocene structure contrasts with the exchange kinetics of these systems at metal electrodes. In the latter environment, uniformly facile kinetics are obtained that apparently exhibit a strong dependence upon the solvent dynamics, indicative of essentially adiabatic behavior.[5a,6b,7] The likelihood that this behavior persists for ferrocenium–ferrocene couples at electrodes, even in solvents such as acetonitrile,[7] suggests that electrochemical exchange processes may follow inherently more adiabatic pathways than for related self-exchange reactions. Indeed, such a conclusion is in harmony with the prediction of recent theoretical treatments.[63]

Although detailed theoretical calculations of H°_{12} have been undertaken so far for only a relatively narrow range of homogeneous-phase self-exchange reactions,[2] most values are below the magnitude, $\lesssim$0.2 kcal mol^{-1}, necessary to maintain a degree of reaction adiabaticity in dynamically rapid solvents, such as water. At least in homogeneous solution, then, the range of outer-sphere reactions influenced importantly by solvent friction effects may well be smaller than those subject primarily to electron-tunneling control of the barrier-crossing frequency. Although the present solvent-dependent analysis is applicable only in unusually favorable circumstances, it would be of considerable interest to utilize it to explore electronic coupling factors in other types of processes, especially involving intramolecular electron transfer.

Acknowledgment. We are grateful to Dr. Marshall Newton for providing details of his matrix element calculations for metallocenes prior to publication. Helpful discussions with Dr. David Beretan, along with preprints of ref 12, contributed significantly to the rate–friction analysis. The NMR instruments used in this work are supported by National Institutes of Health Grant RR01077 and National Science Foundation Grant BBS-8714258 at Purdue University. This research program is supported by the Office of Naval Research.

Appendix

A key element in obtaining the calculated k'_{ex} values, k'_{ex}(calcd), shown in Figure 2 involves the computation of unimolecular rate constants, $k_{et}(r)$, that span the full range from entirely nonadiabatic to adiabatic behavior. For this purpose, we use the following relation, derived in ref 11b:

$$k_{et}(r) = \frac{\tilde{\kappa}_{el} k^{TST}}{1 - \tilde{\kappa}_{el} + [\tilde{\kappa}_{el} k^{TST}/k^a_{et}(r)]} \quad \text{(A1)}$$

where $k^a_{et}(r)$ is the rate constant for adiabatic barrier crossing, and k^{TST} is the rate constant corresponding to the TST limit (i.e., in the absence of solvent friction) given by

$$k^{TST} = (\omega_0/2\pi) \exp(-\Delta G^*/RT) \quad \text{(A2)}$$

where ω_0 is the solvent inertial frequency. The electronic transmission coefficient, $\tilde{\kappa}_{el}$, can be related to the more familiar κ_{el} in eq 1 by[11b]

$$\kappa_{el} = \tilde{\kappa}_{el}/[\kappa_a + \tilde{\kappa}_{el}(1 - \kappa_a)] \quad \text{(A3)}$$

where the "adiabatic transmission coefficient" $\kappa_a = k^a_{et}/k^{TST}$.

Apart from the additional $-\tilde{\kappa}_{el}$ term in the denominator, eq A1 is similar to or identical with other literature relations for interpolating between the adiabatic and nonadiabatic limits (e.g., ref 12 and 13). This term allows $k_{et}(r)$ to reduce to the correct adiabatic TST limit, whereupon the preexponential factor equals $\omega_0/2\pi$.[11b]

The adiabatic rate constant k^a_{et} was calculated by using a position (q)-dependent diffusional model, whereby the diffusion coefficient, D, describing progress along the reaction coordinate in the presence of solvent friction within the intersection region differs from that in the potential energy wells as a result of barrier-top roundedness (i.e., $H_{12} > 0$).[11b] Specifically, k^a_{et} was approximated by

$$(k^a_{et})^{-1} = 2\int_0^{q^*} dq\, [D(q)\, P_{eq}(q)]^{-1} \quad \text{(A4)}$$

where the integration is performed from the reactant well to the barrier top; $P_{eq}(q)$ is given by

$$P_{eq}(q) \approx (2\pi/\beta\omega_0^2)^{1/2} \exp[-\beta V(q)] \quad \text{(A5)}$$

where $\beta = (k_B T)^{-1}$ (k_B is the Boltzmann constant) and $V(q)$ describes the potential energy surface. Appropriate expressions for $D(q)$ in terms of τ_L (i.e., for Debye solvents) and for $V(q)$ are given in ref 11b, along with other pertinent details. The effect of increasing H_{12} is to decrease k^a_{et}; typically k^a_{et} decreases by 2–3-fold as H_{12} increases from 0 to 1 kcal mol^{-1}, the effect depending somewhat on the extent of solvent friction. The results are numerically similar to those obtained[11a] by utilizing the Smoluchowski treatment of Calef and Wolynes[14] or from the more general approach outlined in ref 25. (Note that the effect of solvent friction upon k_{et}, as given by eq A1, is contained entirely within the k^a_{et} term.)

The $\tilde{\kappa}_{el}$ values were calculated by using the approximate expression[11b]

$$\tilde{\kappa}_{el} = 4\pi^{3/2}\gamma_T/(1 + 4\pi^{3/2}\gamma_T) \quad \text{(A6)}$$

where

$$\gamma_T = |H_{12}|^2/4\hbar\omega_0(\Delta G^* k_B T)^{1/2} \quad \text{(A7)}$$

For the present purposes, it is most important to note that the derived values of $\tilde{\kappa}_{el}$, and hence the form of the log k_{ex}(calcd)–log τ_L^{-1} curves in Figure 2, are insensitive to the particular expression used for $\tilde{\kappa}_{el}$.[11b]

Supplementary Material Available: Table of ^{1}H NMR parameters and related data for metallocene self-exchange (2 pages). Ordering information is given on any current masthead page.

(58) For example: (a) Hammett, L. P. *Physical Organic Chemistry*; 2nd ed.; McGraw-Hill: New York, 1968. (b) Ritchie, C. D.; Sager, W. F. *Prog. Phys. Org. Chem.* **1964**, *2*, 323.

(59) (a) Hall, D. W.; Russell, C. D. *J. Am. Chem. Soc.* **1967**, *89*, 2316. (b) Little, W. F.; Reilley, C. N.; Johnson, J. D.; Sanders, A. P. *J. Am. Chem. Soc.* **1964**, *86*, 1382. (c) Kuwana, T.; Bublitz, D. E.; Hoh, G. *J. Am. Chem. Soc.* **1960**, *82*, 5811.

(60) Sparser data for cobaltocene couples are given in: El Murr, N. *Transition Met. Chem.* **1981**, *6*, 321.

(61) Butter, S. A.; Beachell, H. C. *Inorg. Chem.* **1966**, *5*, 1820.

(62) A general influence of altering the overall electron density to the orbital overlap of the HOMO–LUMO pair might nevertheless be anticipated since the removal of the electron from the HOMO will cause alterations in the remaining electronic energy states. The implications of this "charge relaxation effect" upon H_{12} are addressed in ref 2c,d.

(63) (a) Morgan, J. D.; Wolynes, P. G. *J. Phys. Chem.* **1987**, *91*, 874. (b) Zusman, L. D. *Chem. Phys.* **1987**, *112*, 53.

(64) Press, W. H.; Flannery, B. P.; Tenkolsky, S. A.; Vetterling, W. T. *Numerical Recipes*; Cambridge University Press: Cambridge, U.K., 1986; pp 126–130.